

# Analyses of the Pinning Mechanism for the Superconductor/Normal-Metal and Superconductor/Superconductor Multilayers

Y. Obi,<sup>1</sup> M. Ikebe,<sup>2</sup> and H. Fujishiro<sup>2</sup>

Published online: 3 August 2006

The vortex pinning force of superconductor(S)/normal-metal(N) multilayers, Nb/Ti and Nb<sub>100-x</sub>Ti<sub>x</sub>/Ti, and superconductor(S)/superconductor(S') multilayers, Nb<sub>100-x</sub>Ti<sub>x</sub>/Nb and Nb<sub>28</sub>Ti<sub>72</sub>/Nb<sub>65</sub>Ti<sub>35</sub>, has been studied as a function of the layer thickness  $d$  for various compositions of  $x$ . The transverse pinning force density  $F_{p\perp}$  acting perpendicular to the layer planes makes a peak around  $d \sim 2\xi_{GL}$  ( $\xi_{GL}$ : the GL coherence length) for both the S/N and S/S' multilayers, where they exhibit the quasi-two-dimensional superconductivity. In contrast, the longitudinal pinning force density  $F_{p\parallel}$  acting parallel to the layer plane hardly depends on  $d$ . The pinning mechanism inherent in the layered structure has been analyzed based on the GL free energy, which clarified that the effective pinning force due to the multilayer structure originates from the difference in the potential energy for the S/N multilayer and from the difference in the kinetic energy for the S/S' multilayer between the constituent layers. The  $d$  dependence of the  $F_{p\perp}$ , however, has been found to be qualitatively similar for the S/N and S/S' multilayers.

**KEY WORDS:** multilayer; superconductor; critical current; pinning force.

## 1. INTRODUCTION

The superconducting properties of the superconductor(S)/normal-metal(N) and superconductor(S)/superconductor(S') multilayers are quite unique and interesting, both type multilayers showing characteristic dimensional crossover in case of  $d \sim 2\xi_{GL}$  ( $d$ : sublayer thickness,  $\xi_{GL}$ : the GL coherence length) [1] as is known as quasi-two-dimensional superconductivity. Divided by the dimensional crossover temperature  $T_D$ , the dimensionality of superconductivity under the applied field parallel to the layer plane  $H_{\parallel}$  changes from three-dimensional(3D) for  $T_D < T < T_c$  ( $T_c$ : superconducting transition temperature) to 2D for  $T < T_D$  with decreasing temperature  $T$ . In the 3D-superconductivity region above  $T_D$ , the size of

the vortex is large and extends over the several sublayers. However, the nature of the 2D superconductivity below  $T_D$  is different between the S/N and S/S' multilayers. In the S/N multilayer under  $H_{\parallel}$ , the fluxoids are stabilized in the N layer, while in the S/S' layer, the fluxoids are stabilized in the S layer with shorter  $\xi_{GL}$ .

The flux pinning characteristics for the multilayered materials are very attractive subjects because the multilayer structure itself is considered to play an essential role as a pinning center [2]. In the multilayers, the transverse pinning force density  $F_{p\perp}$  acting in the perpendicular direction to the layer is much enhanced compared to the longitudinal pinning force density  $F_{p\parallel}$  [3] acting parallel to the layer. In the S/N multilayers, the N layer works as an attractive pin center. The fluxoids are stabilized in the N layer and the difference in the potential energy between the S and N sublayers, i.e., the loss of the superconducting condensation energy due to the vortex formation in the S layer, is considered to be the main origin

<sup>1</sup>Institute for Materials Research, Tohoku University, Sendai 980-8577, Japan; e-mail: obi@imr.tohoku.ac.jp.

<sup>2</sup>Faculty of Engineering, Iwate University, Morioka 020-8551, Japan.

of enhanced  $F_{p\perp}$ . In contrast, for the S/S' multilayer such as NbTi/Nb with almost the same condensation energy of the S and S' layer, the main origin of  $F_{p\perp}$  is to come from the kinetic energy term of the GL free energy between S and S', which stabilizes the vortices in the superconducting layer with shorter  $\xi_{GL}$  [4,5].

The transverse pinning force density  $F_{p\perp}$  is usually strongly dependent on the structural modulation length  $\lambda$ . In case of the multilayer structure of this study with equal sublayer thickness ( $\lambda = 2d$ ), the  $F_{p\perp}$  value has been found to take the maximum around  $d \sim 2\xi_S$ , for both the S/N and S/S' multilayers. This result may originate from a kind of the matching effect between the vortex size and the layer thickness. We have investigated [6] the difference of the pinning force between the S/N and S/S' multilayers and found that the behavior of the pinning force as a function of  $\lambda$  is qualitatively much similar in both systems despite the different type (superconducting S' or normal-metal N) intervening layers.

In this paper, we investigate  $F_{p\perp}$  of S/N and S/S' multilayers with different  $\xi_{GL}$  and  $\lambda$  values. We examine the pinning mechanism for the S/N and S/S' multilayers, taking into account the difference in the GL potential energy and/or the GL kinetic energy between the constituent layers. We discuss the strength of the  $F_{p\perp, \max}$ , the maximum value of  $F_{p\perp}$  as a function of applied field  $H_{\parallel}$ , with respect to the coherence length  $\xi_{GL}$ . We also argue the  $\lambda$  dependence of  $F_{p\perp, \max}$ .

## 2. EXPERIMENTAL

Superconductor(S)/normal-metal(N) and superconductor(S)/superconductor(S') multilayers have been fabricated by an RF dual sputtering onto quartz substrates. Samples of each series are composed of Nb/Ti and  $\text{Nb}_{100-x}\text{Ti}_x/\text{Ti}$  ( $\text{Nb}_{65}\text{Ti}_{35}/\text{Ti}$ ,  $\text{Nb}_{50}\text{Ti}_{50}/\text{Ti}$  and  $\text{Nb}_{28}\text{Ti}_{72}/\text{Ti}$ ) for S/N and  $\text{Nb}_{100-x}\text{Ti}_x/\text{Nb}$  ( $\text{Nb}_{65}\text{Ti}_{35}/\text{Nb}$ ,  $\text{Nb}_{50}\text{Ti}_{50}/\text{Nb}$  and  $\text{Nb}_{28}\text{Ti}_{72}/\text{Nb}$ ) and  $\text{Nb}_{28}\text{Ti}_{72}/\text{Nb}_{65}\text{Ti}_{35}$  for S/S' multilayers. Samples were designed so as to have an equal sublayer thickness,  $d_S = d_N = d = (1/2)\lambda$  and  $d_S = d_{S'} = d = (1/2)\lambda$ , where  $d_S$ ,  $d_N$  and  $d_{S'}$  are the thickness of the S, N and S' sublayer and  $\lambda$  is the structural modulation wavelength. The total sample thickness was designed to be about 5000 Å. The critical current density ( $J_c$ ) was measured resistively with the current parallel to the layer at 1.5 K under the magnetic field parallel ( $J_c(H_{\parallel})$ ) and perpendicular to the layer plane ( $J_c(H_{\perp})$ ). The transverse pinning force density  $F_{p\perp}$

and longitudinal pinning force density  $F_{p\parallel}$  were estimated from the critical current density  $J_c$  by the relations,  $F_{p\perp} = (1/c)J_c(H_{\parallel}) \times H_{\parallel}$  and  $F_{p\parallel} = (1/c)J_c(H_{\perp}) \times H_{\perp}$ ,  $H_{\parallel}$  and  $H_{\perp}$  being applied fields parallel and perpendicular to the layer and  $c$  being the light velocity.

## 3. RESULTS AND DISCUSSION

Figure 1 shows the critical current density  $J_c(H_{\parallel})$  and  $J_c(H_{\perp})$  at 1.5 K for  $\text{Nb}_{65}\text{Ti}_{35}/\text{Ti}$  as the typical case of S/N (Fig. 1a) and for  $\text{Nb}_{65}\text{Ti}_{35}/\text{Nb}$  as the typical case of S/S' (Fig. 1b) with various modulation wavelengths. In this figure, it is clear that for both samples  $J_c(H_{\perp})$  hardly depends on  $\lambda$ , while  $J_c(H_{\parallel})$  heavily depends on  $\lambda$  and has higher values compared to  $J_c(H_{\perp})$ . Although  $J_c(H = 0)$  is rather high for S/S' relative to S/N,  $J_c(H_{\parallel})$  is more enhanced for

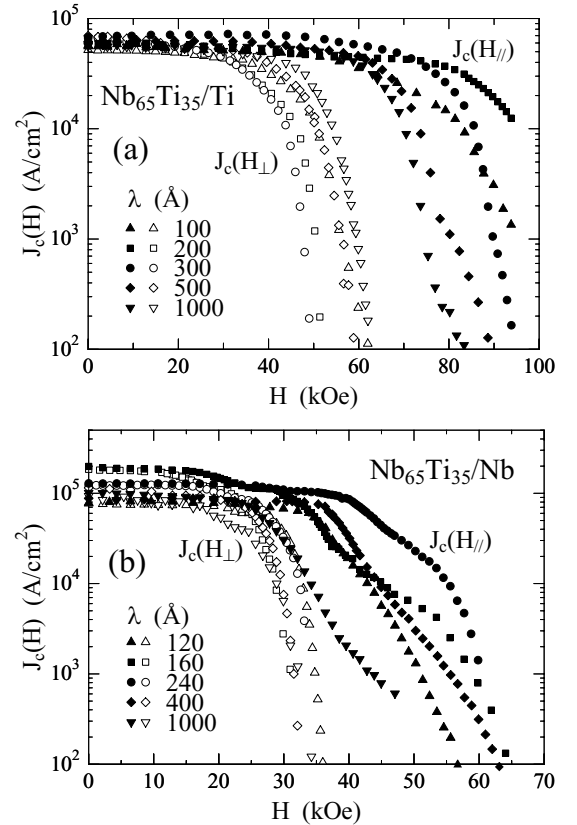


**Fig. 1.**  $J_c(H_{\parallel})$  and  $J_c(H_{\perp})$  at 1.5 K for the typical example of the present S/N and S/S' multilayers as a function of the modulation wavelength  $\lambda$ . (a)  $\text{Nb}_{65}\text{Ti}_{35}/\text{Ti}$  and (b)  $\text{Nb}_{65}\text{Ti}_{35}/\text{Nb}$ . In both the figures open symbols denote the  $J_c(H_{\perp})$  and closed symbols denote the  $J_c(H_{\parallel})$ .

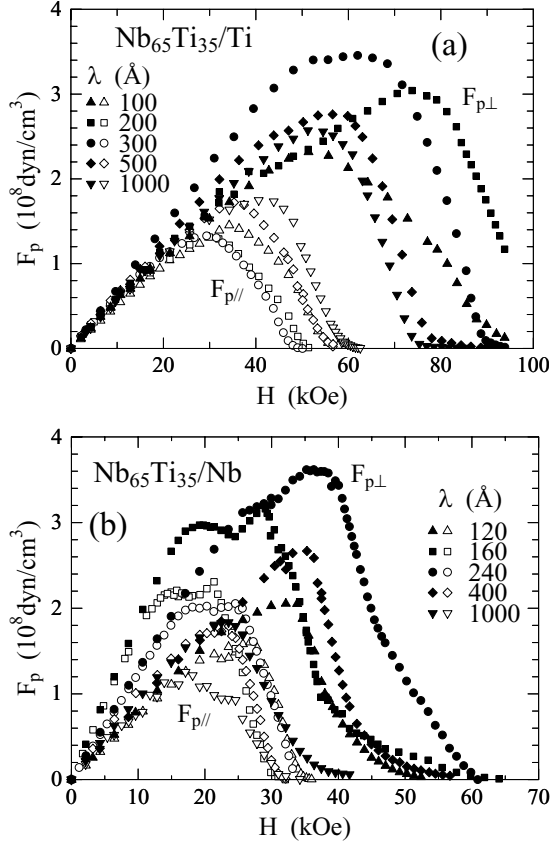


**Fig. 2.** Transverse pinning force density  $F_{p\perp}$  as a function of parallel field  $H_{\parallel}$  and longitudinal pinning force density  $F_{p\parallel}$  as a function of perpendicular field  $H_{\perp}$  at 1.5 K for (a) Nb<sub>65</sub>Ti<sub>35</sub>/Ti and (b) Nb<sub>65</sub>Ti<sub>35</sub>/Nb with various  $\lambda$  values. *Open symbols* denote  $F_{p\parallel}$  and *closed symbols* denote  $F_{p\perp}$ .

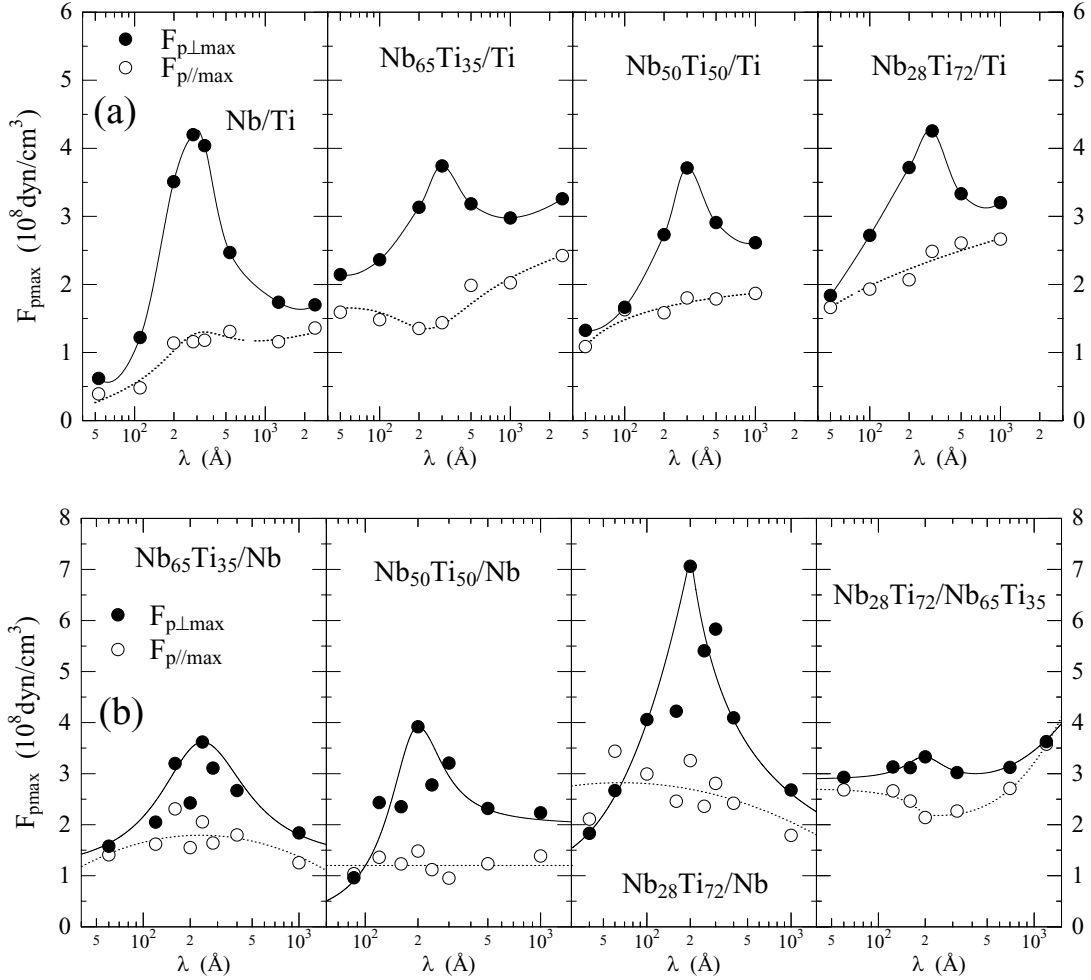
S/N than S/S' in high magnetic field region because of the higher parallel critical field  $H_{c2\parallel}$  of the S/N multilayer [3].

Figure 2 presents the macroscopic transverse pinning force density  $F_{p\perp}$  and the macroscopic longitudinal pinning force density  $F_{p\parallel}$  as a function of the applied magnetic field at 1.5 K for the same samples as Fig. 1. The characteristic features are as follows:  $F_{p\parallel}$  is always smaller compared to  $F_{p\perp}$  for both the S/N and S/S' multilayer series and  $F_{p\perp}$  is very sensitive to the modulation wavelength  $\lambda$  for the both series, i.e.,  $F_{p\perp}$  is rather small at small and large  $\lambda$  values but it is enhanced at the medium  $\lambda$  region. On the other hand, the longitudinal pinning force  $F_{p\parallel}$  is nearly independent of  $\lambda$ . This implies that for the perpendicular direction, the layer structure is intrinsically involved in the pinning mechanism as expected, while for the parallel direction, the size of layer thickness does not directly affect the pinning force.

Figure 3 shows the maximum transverse pinning force density  $F_{p\perp\max}$  and the maximum longitudinal pinning force density  $F_{p\parallel\max}$  at 1.5 K as a function of  $\lambda$  for the S/N (Fig. 3a) and S/S' multilayers (Fig. 3b), respectively.  $F_{p\max}$  is defined as the maximum value of  $F_p$  versus  $H$  curve for each sample.  $F_{p\perp\max}$  takes a broad peak around  $\lambda = 200$ – $300$  Å for all the samples of both the S/N and S/S' series studied. In contrast,  $F_{p\parallel\max}$  does not have a definite  $\lambda$ -dependence but all the  $F_{p\parallel\max}$  values for S/N series slightly increase with increasing  $\lambda$ . In the case of  $F_{p\parallel}$ , vortices penetrate perpendicular to the layer planes and move parallel to the layer plane. So this slight increase of  $F_{p\parallel\max}$  suggests the growing up of the local pin inside of the superconducting NbTi layer with the increase of the layer thickness. In the case of S/S' multilayers, the slight increase of  $F_{p\parallel\max}$  is not discernible and the  $F_{p\parallel\max}$  data scatter may come from the different sample quality which yields the different size of local pinning center. We assume that these local pins may act isotropically in the multilayers.

In order to estimate correctly the net pinning force working only in the perpendicular direction, it is necessary to eliminate the influence of the sample dependent isotropic local pins. We define the effective transverse pinning force density  $F_{pL}$  by  $F_{pL} = F_{p\perp} - F_{p\parallel}$ , which is to describe the pinning force inherent to the layer structure. The results of  $F_{pL\max}$  ( $= F_{p\perp\max} - F_{p\parallel\max}$ ) are shown in Fig. 4 as a function of  $d/2\xi_S$  ( $\xi_S$ :  $\xi_{GL}$  of the S layer) for the S/N (Fig. 4a) and the S/S' (Fig. 4b) multilayer series. Here we have set  $\xi_S$  at  $T = 1.5$  K as 100.0, 63.4, 58.9 and 42.4 Å for Nb, Nb<sub>65</sub>Ti<sub>35</sub>, Nb<sub>50</sub>Ti<sub>50</sub> and Nb<sub>28</sub>Ti<sub>72</sub>, respectively [7]. In these figures, the layer thickness is normalized with respect to  $2\xi_S$  because the core size of the vortex should approximately be  $2\xi_S$ . As schematically pictured in Fig. 5, the results of Fig. 4 suggest that the layer structure works most effectively as a pinning center at around  $d \sim 2\xi_S$  possibly because of the matching effect between the S thickness and the size of the vortex core. It is also to be noticed that  $d/2\xi_S \sim 1$  corresponds to the typical case of the quasi-2D state for the superconductivity of the multilayer system [3].

In Fig. 4a and b, the peak value of  $F_{pL\max}$  as a function of  $d/2\xi_S$ , which we define as  $M(F) = [F_{pL\max}]_{\max}$ , depends on the alloy composition of the S layer of each series and the difference of the size of the GL coherence length may be the origin of the composition dependence of  $M(F)$ . In order to estimate the size of  $M(F)$ , it is useful to start from the



**Fig. 3.** Maximum pinning force for the transverse direction  $F_{p\perp\max}$  (closed circles) and longitudinal direction  $F_{p\parallel\max}$  (open circles) as a function of  $\lambda$  for (a) S/N series and (b) S/S' series. Lines are the guide to the eyes.

following equation of the GL free energy  $F_s$ ,

$$F_s = F_n(0) + \alpha|\Psi|^2 + (\beta/2)|\Psi|^4 + (1/2m^*) |(-i\hbar\nabla - 2e\mathbf{A})\Psi|^2 + (1/2\mu_0)(\text{rot}\mathbf{A})^2 \quad (1)$$

where  $F_n(0)$  is the free energy of the normal state in the absence of magnetic field,  $\Psi$  the order parameter,  $m^*$  the mass of superconducting electron,  $\mu_0$  the permeability of vacuum,  $\mathbf{A}$  the vector potential, and  $\alpha$  and  $\beta$  are the numerical coefficients. The calculation for the pinning force has been performed by Matsushita [8] for S/N multilayer taking account of the difference of potential energy between the normal and the superconducting layers. The elementary transverse pinning force  $f_{p\perp}$  by a boundary is

given by

$$f_{p\perp} \sim 0.305\pi\mu_0 H_c^2 \xi_S \quad (2)$$

where  $H_c$  is the thermodynamical critical field. In the case of S/S' multilayer with nearly the same  $H_c$ , we have calculated the elementary pinning force by a boundary due to the difference of kinetic energy between S and S' layer in a previous paper [7] and have got the following relation,

$$f_{p\perp} \sim 0.612\pi\mu_0 H_c^2 (\xi_{S'} - \xi_S), \quad (3)$$

where  $\xi_{S'}$  is  $\xi_{GL}$  of the S' layer (Nb and  $\text{Nb}_{65}\text{Ti}_{35}$  in the present case). Thus in the S/N multilayers, the transverse elementary pinning force should be proportional to  $\xi_S$ , while it is to be proportional to  $(\xi_{S'} - \xi_S)$  in the S/S' layer. In Fig. 6, we plot  $M(F)$

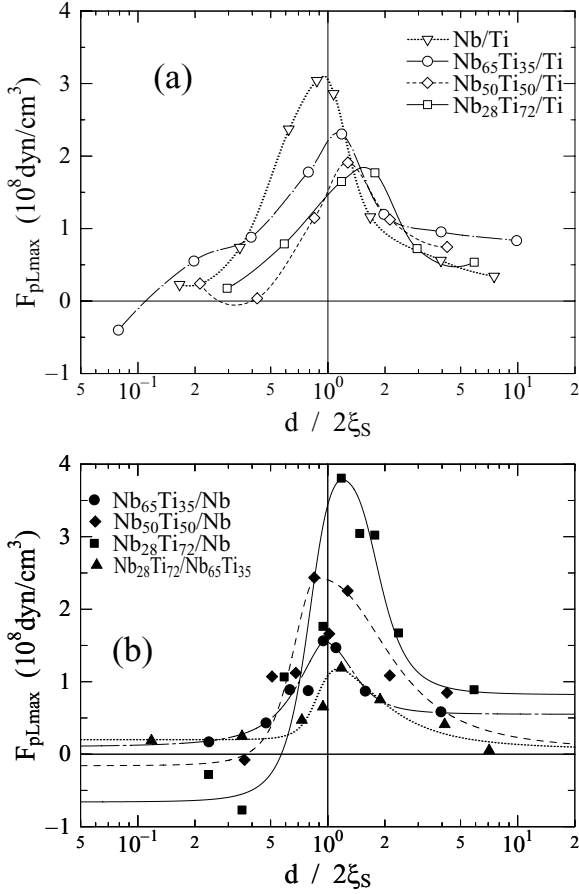


**Fig. 4.**  $F_{pL,max}$  ( $= F_{p\perp,max} - F_{p\parallel,max}$ ) for (a) S/N and (b) S/S' multilayers as a function of  $d/2\xi_S$ , where  $\xi_S$  is  $\xi_{GL}$  of the S layer. Lines are the guide to the eyes.

versus  $\xi_S$  (Fig. 6a) for all the S/N layers and  $M(F)$  versus  $(\xi_{S'} - \xi_S)$  (Fig. 6b) for all the S/S' layers studied. In these figures,  $M(F)$  can be confirmed to be roughly proportional to  $\xi_S$  for the Nb/Ti and NbTi/Ti multilayers and to  $(\xi_{S'} - \xi_S)$  for the NbTi/Nb and NbTi/NbTi multilayers. These results suggest that for  $M(F)$ , satisfying the ideal size matching condition between the layer thickness and the vortex core, the elementary pinning force  $f_{p\perp}$  is of vital importance for the observed pinning force strength and that the main origin for the vortex pinning is actually the condensation energy for S/N and the kinetic energy for the S/S' system. In both systems, the boundary pin plays the main role for the pinning mechanism to determine the maximum pinning force density  $M(F)$ .

Next, let us briefly argue the macroscopic pinning strength as a function of the layer thickness  $d$ . As mentioned above, the effective transverse pinning

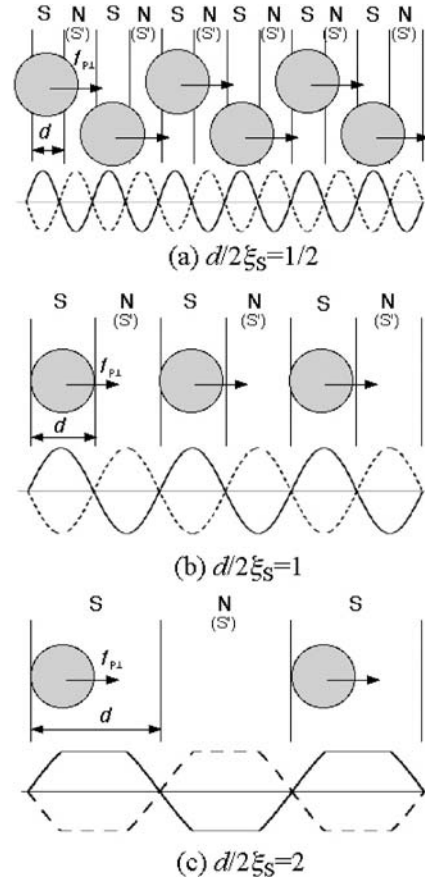


**Fig. 5.** Schematic representation of the layer structure and the vortex core size. The arrows indicate the direction of the elementary pinning force  $f_{p\perp}$ . The vortex energy as a function of the vortex center position is qualitatively given by the solid lines for S/N and by dashed lines for S/S' multilayers below each figure.

force density  $F_{pL}$  makes the maximum at  $d \sim 2\xi_S$ . Even in the region of  $d > 2\xi_S$  or  $d < 2\xi_S$ , the S-N or S-S' boundary should vitally influences on  $F_{pL}$  ( $= F_{p\perp} - F_{p\parallel}$ ) because  $F_{pL}$  remains positive irrespective of the  $d/2\xi_S$  values.  $F_{pL}$  is naturally expected to be proportional to the pin density, i.e., the number density  $N$  of the boundary. On the other hand, the elementary pinning force  $f_{p\perp}$  is to become not fully effective for  $d < 2\xi_S$  because of the layer size of the vortex core extending over several sublayers. We introduce the efficiency factor  $\varepsilon$  ( $0 \leq \varepsilon \leq 1$ ). The effective transverse pinning force density is written as

$$F_{pL} = N\varepsilon f_{p\perp}. \quad (4)$$

For  $d \geq 2\xi_S$ ,  $\varepsilon$  is constant ( $\varepsilon = 1$ ). For  $d < 2\xi_S$ ,  $\varepsilon$  was pointed out to decrease with decreasing  $d$  as  $\varepsilon \propto (d/2\xi_S)^2$  by Kramer *et al.* [9]. The pin density  $N$  may

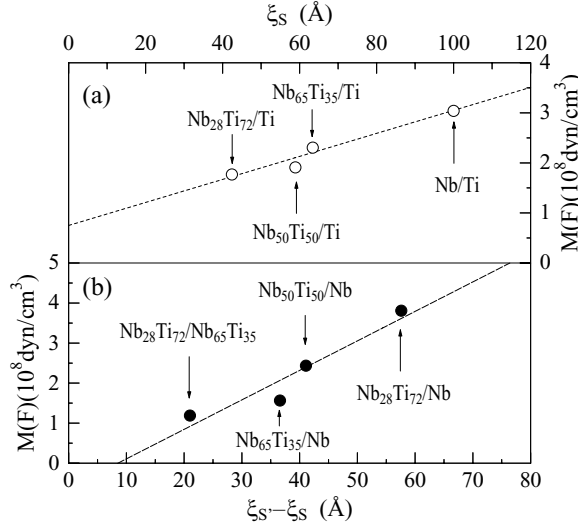


**Fig. 6.**  $M(F)$  ( $= [F_{pL,max}]_{max}$ ) as a function of (a)  $\xi_S$  for S/N and as a function of (b)  $\xi_{S'} - \xi_S$  for S/S' multilayer. *Straight lines* are the result of the least square fitting.

be equal to  $1/d$  over the entire region of  $d/2\xi_S$ . Therefore, the following relations are expected to hold:

$$F_{pL} \propto df_{p\perp} \quad \text{for } d < 2\xi_{GL} \quad (5a)$$

$$F_{pL} \propto f_{p\perp}/d \quad \text{for } d \geq 2\xi_{GL} \quad (5b)$$

The effective transverse pinning force density has the peak around the typical quasi-2D superconductivity region in accord with Eq. (5), where the vortex size just fits the S layer thickness ( $d = 2\xi_S$ ). In

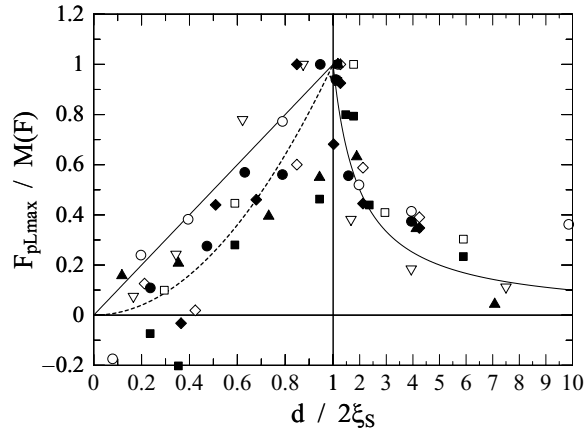


**Fig. 7.** Normalized  $F_{pL,max}$  value ( $= F_{pL,max}/M(F)$ ) as a function of  $d/2\xi_S$  for all the present multilayers. Each symbol has the same meaning as that in Fig. 4. Two *solid lines* show  $F_{pL,max}/M(F) = d/2\xi_S$  for  $d < 2\xi_S$  and  $F_{pL,max}/M(F) = 2\xi_S/d$  for  $d \geq 2\xi_S$ . The *dashed line* for  $d < 2\xi_S$  presents  $F_{pL,max}/M(F) = (d/2\xi_S)^2$ .

Fig. 7, we present the normalized maximum pinning force  $F_{pL,max}/M(F)$  as a function of  $d/2\xi_S$  for all the present S/N and S/S' multilayers. In the figure, the solid linear line for  $d \leq 2\xi_S$  and  $1/d$  curve for  $d \geq 2\xi_S$  correspond to Eqs. (5a) and (5b), respectively. The experimental results for both the N/S (open symbols) and S/S' (closed symbols) systems follow pretty well the predicted  $1/d$  line of Eq. (5b) for  $d \geq 2\xi_S$ . In the region of  $d < 2\xi_S$ , the experimental points for the S/N system seem to roughly follow the  $d$ -linear line of Eq. (5a). However, the data points for the S/S' system are more scattered and seem to follow rather the  $(d/2\xi_S)^2$  dashed line. The calculation of Kramer *et al.* which obtained  $\varepsilon = (d/2\xi_S)^2$  relation is based on the proximity effect and assumes the S/N layer structure and might not be applicable to the S/S' system. Another possibility for the failure of the Eq. (5a) for the S/S' system might come from the estimation of the pin number density  $N$ . In the S/S' multilayers for  $d < 2\xi_S$ ,  $N$  might not be well-defined in terms of the layer boundary and the relation  $N = 1/d$  might not be valid, making  $F_{pL}$  directly proportional to  $\varepsilon f_{p\perp} \propto d^2 f_{p\perp}$ .

#### 4. SUMMARY

We have investigated and analyzed the mechanisms of pinning force for the superconductor/normal-metal (S/N: S = Nb, Nb<sub>65</sub>Ti<sub>35</sub>, Nb<sub>50</sub>Ti<sub>50</sub>, Nb<sub>28</sub>Ti<sub>72</sub>, N = Ti) and superconductor/superconductor (S/S': S = Nb<sub>65</sub>Ti<sub>35</sub>, Nb<sub>50</sub>Ti<sub>50</sub>, Nb<sub>28</sub>Ti<sub>72</sub>, S' = Nb, Nb<sub>65</sub>Ti<sub>35</sub>) multilayers having equal thickness  $d$  of each sublayer for various structural wavelength  $\lambda$  ( $=2d$ ). For all the multilayer samples of S/N and S/S', the effective transverse pinning force density  $F_{pL,max}$  makes the peak at  $d \cong 2\xi_S$  ( $=GL$  coherence length of the S layer) and decreases as  $F_{pL,max} \propto 2\xi_S/d$  for  $d > 2\xi_S$  in accord with the decrease of the transverse pin density  $N$  ( $=$ number density of the layer boundary). For  $d < 2\xi_S$ ,  $F_{pL,max}$  of the S/N multilayers decreased roughly as  $F_{pL,max} \propto d/2\xi_S$  in accord with the efficiency factor  $\varepsilon$  ( $\propto (d/2\xi_S)^2$ ) calculated by Kramer *et al.* for the S/N multilayer system based on the proximity effect. The data points of  $F_{pL,max}$  of the S/S' system are somewhat scattered but seems to decrease rather as  $F_{pL,max} \propto (d/2\xi_S)^2$ , i.e., directly proportional to  $\varepsilon$ , making a marked contrast to the S/N system.

$M(F)$ , defined as the maximum value of  $F_{pL,max}$  for each series has the linear relation with respect to  $\xi_S$  for the S/N and to the  $\xi_{S'} - \xi_S$  for the S/S' multilayers. These results clearly support

that the boundary pin arising from the difference in the potential energy is of essential importance for the S/N system and the boundary pin arising from the difference in the kinetic energy is of essential importance for the S/S' system as a pinning mechanism.

## REFERENCES

1. S. Takahashi and M. Tachiki, *Phys. Rev. B* **34**, 3162 (1986).
2. M. Tachiki and S. Takahashi, *Solid State Commun.* **70**, 291 (1989).
3. Y. Obi, S. Takahashi, H. Fujimori, M. Ikebe, and H. Fujishiro, *J. Low Temp. Phys.* **96**, 1 (1994).
4. K. Matsumoto, H. Takewaki, Y. Tanaka, O. Miura, K. Yamafuji, K. Funaki, M. Iwakuma, and T. Matsushita, *Appl. Phys. Lett.* **64**, 115 (1994).
5. T. Matsushita, M. Iwakuma, K. Funaki, K. Yamafuji, K. Matsumoto, O. Miura, and Y. Tanaka, *Adv. Cryog. Eng.* **42**, 1103 (1996).
6. Y. Obi, H. Fujimori, M. Ikebe, and H. Fujishiro, *Superlattices Microstruct.* **21**, 423 (1997).
7. Y. Obi, M. Ikebe, and H. Fujishiro, *J. Low Temp. Phys.* **137**, 125 (2004).
8. T. Matsushita, *Magnetic Flux Pinning and Electromagnetic Phenomena* (Sangyo-Tosho, Tokyo, Japan, 1994), p. 236.
9. E. J. Kramer and H. C. Freyhardt, *J. Appl. Phys.* **51**, 4930 (1980).